



In silico investigation of cannabinoids from *Cannabis sativa* leaves as a potential anticancer drug to inhibit MAPK-ERK signaling pathway and EMT induction

Shabnoor Iqbal¹ · Motlalepula Matsabisa¹

Received: 15 February 2024 / Accepted: 15 April 2024
© The Author(s) 2024

Abstract

Genes related to MAPK-ERK signaling pathways, and epithelial-mesenchymal transition induction is evolutionarily conserved and has crucial roles in the regulation of important cellular processes, including cell proliferation. In this study, six cannabinoids from *Cannabis sativa* were docked with MAPK-ERK signaling pathways to identify their possible binding interactions. The results showed that all the cannabinoids have good binding affinities with the target proteins. The best binding affinities were MEK- tetrahydrocannabinol (– 8.8 kcal/mol) and P13k-cannabinol (– 8.5 kcal/mol). The root mean square deviation was calculated and used two alternative variants (rmsd/ub and rmsd/lb) and the values of rmsd/lb fluctuated 8.6–2.0 Å and for rmsd/ub from 1.0 to 2.0 Å that suggests the cannabinoids and protein complex are accurate and cannot destroy on binding. The study analyzed the pharmacokinetic and drug-likeness properties of six cannabinoids from *C. sativa* leaves using the SwissADME web tool. Lipinski's rule of five was used to predict drug-likeness and showed that all compounds have not violated it and the total polar surface area of cannabinoids was also according to Lipinski's rule that is benchmarked of anticancer drugs. Cannabinoids are meet the requirements of leadlikeness and synthetic accessibility values showed they can be synthesized. The molecular weight, XLOGP3, solubility (log S), and flexibility (FLEX) are according to the bioavailability radar. The bioavailability score and consensus Log Po/w fall within the acceptable range for the suitable drug. Pharmacokinetics parameters showed that cannabinoids cannot cross the blood–brain barrier, have high GI absorption as well as cannabinoids are substrates of (CYP1A2, CYP2C19, CYP2C9, CYP2D6, and CYP3A4) but no substrate of P-glycoprotein. Based on these findings, the study suggests that cannabinoids are suitable drugs that could be used as effective inhibitors for target proteins involved in cancer pathways. Among the six cannabinoids, cannabinol and tetrahydrocannabinol exerted maximum binding affinities with proteins of MAPK-ERK signaling pathways, and their pharmacokinetics and drug-likeness-related profiles suggest that these cannabinoids could be superlative inhibitors in cancer treatment. Further in vitro, in vivo, and clinical studies are needed to explore their potential in cancer treatment.

Keywords Cannabinoids · Cannabis · Cancer · Protein kinase · Mitogen-activated protein kinase · Epithelial to mesenchymal transition

Introduction

Numerous blockbuster medicines are produced, either directly or indirectly, from plants, which are the major source of novel pharmacologically active chemicals (Dehelean

et al. 2021). Plants play a vital role in the treatment and prevention of diseases, even in conjunction with synthetic chemistry as a technique of drug discovery and production from plant scaffold molecules. Natural products will remain a vital source of therapeutic medicines. Many other natural products can be used as chemical models or as models for synthesis, and semi-synthesis of new molecules meant to cure human ailments, in addition to the ones that have been shown to have direct medicinal applications (Emhemmed et al. 2022).

The biological process known as the epithelial-to-mesenchymal transition (EMT) is important for several

✉ Shabnoor Iqbal
iqbal.s@ufs.ac.za

¹ AMITD Department of Pharmacology, School of Clinical Medicine, Faculty of Health Sciences, University of the Free State, Bloemfontein 9300, South Africa

physiological and pathological circumstances, including cancer and tissue homeostasis. It converts epithelial cells into mesenchymal cells, which enhances their migratory and invasion potential while decreasing their ability to adhere and undergo apoptosis (Beach et al. 2011; Hamidi et al. 2022). While the EMT process increases cell motility and the production of mesenchymal markers (N-cadherin, fibronectin, and vimentin), it also attenuates cell–cell adhesion and downregulates epithelial indicators (E-cadherin) (Serrano-Gomez et al. 2016). Moreover, it is connected to drug treatment resistance, metastasis, and tumor growth. Through EMT, tumor cells at the primary tumor site can become migratory and invasive, which helps them spread to other organs and eventually metastasis (Pan et al. 2021; Huang et al. 2022). The signaling pathway RAF/MEK/ERK is responsible for controlling various cellular functions, such as cell division, proliferation, motility, and survival. In general, ERK1/2 activation stimulates cell proliferation, and many malignancies are characterized by its dysregulated activity (Sugiura et al. 2021). Additionally, the PI3K/Akt pathway plays a critical role in EMT by triggering downstream effectors that control cellular functions such as invasion, migration, and cell survival (Wei et al. 2019; Navaei et al. 2021). Furthermore, a variety of downstream targets, including transcription factors (FOXOs), cell cycle regulators (p21 and p27), and elements of the mTOR pathway (mTOR and p70S6K), are phosphorylated and regulated by active Akt kinase (Johnson et al. 2010; Farhan et al. 2017).

The usage of innovative psychoactive drugs that contain synthetic cannabinoids is on the rise (Castaneto et al. 2014). Products containing synthetic cannabinoids have effects resembling those of natural cannabis, but they are stronger, more hazardous, and have been linked to harmful side effects. A variety of psychotropic substances, primarily with high-potency cannabinoid receptor binding, are included in synthetic pharmaceuticals. The effects of natural cannabis and Δ^9 -tetrahydrocannabinol are mimicked by these synthetic drugs, but they cause more severe side effects, such as chest pain, tachycardia, anxiety, cognitive impairment, agitation, respiratory difficulties, muscle twitches, acute renal failure, and psychosis (Cohen and Weinstein 2018).

Numerous studies have been conducted on the application of cannabinoids as an anti-cancer treatment. It was found that it generally has beneficial and protective effects, preventing the growth and spread of tumors and reestablishing homeostasis. Therapeutic trials on the use of cannabinoids as an anti-cancer medication are currently being conducted, even though their therapeutic use in palliative care is well documented (Tomko et al. 2020).

It is anticipated that the pharmacokinetic and molecular docking data of cannabinoids and the proteins related to MAPK-ERK signaling pathways will help ensure that these drugs are successfully deciphered and developed into

Table 1 PubChem CIDs of ligands

Sr no	Ligand	PubChem CID
1.	Cannabigerol	5,315,659
2.	Cannabichromene	30,219
3.	Tetrahydrocannabivarin	93,147
4.	Cannabinol	2543
5.	Cannabidiol	644,019
6.	Tetrahydrocannabinol	16,078

Table 2 PDB ID of selected proteins

Sr No	Protein	PDB ID
1	Vimentin	1gk4
2	Akt	1o6l
3	ERK1	2zoq
4	JNK	4yr8
5	mTOR	5flc
6	P13K	5itd
7	P38	5uoj
8	MEK	7juy
9	ERK2	2ERK
10	E-cadherin	4zt1

oncological healthcare since drug repurposing is a much faster and more cost-effective process than the de novo introduction of a new drug into the clinic.

Materials and methods

Ligand preparation

Through the PubChem database, we downloaded cannabinoids as SDF file and saved in “.pdbqt” format using BIOVIA/ Discovery Studio 2021 (Table 1).

Optimization of the proteins

The 3D crystal structure of all the target proteins was downloaded as the Protein Data Bank (PDB) from <https://www.rcsb.org/>. Discovery Studio Visualizer 2021 was run to crystallize the target proteins with ligands. For this, all water molecules, small molecules, and ligands were deleted from the protein crystal structure and the optimized proteins were saved in pdbqt format (Table 2).

Molecular docking analysis

The molecular docking analysis was performed on the PyRx Virtual screening tool (version 0.9) that assesses the suitable binding alignments of the ligands as well as the

targeted proteins. The ligands are docked to the protein surface. Using this information, the optimal orientations of the ligand with the best binding affinities for the protein active sites were determined. Discovery Studio Visualizer 2021 was run to exhibit the ligands and protein binding with the respective amino acid residues. Based on the lowest binding affinities needed for the binding ligand to attach to the protein, the optimal poses were selected. The binding box of protein-ligands was built in Auto Dock software. The binding box-related files were analyzed in Auto Dock Vina built-in PyRx software, and PDBQT files were created.

Homology modeling for Protein structure validation

Homology modeling was performed to validate the structure of the optimized protein data bank before molecular docking. A program called PROCHECK was used to validate modeled proteins. PROCHECK generates a Ramachandran plot and assesses the atomic distances, surface area, bond angle, and torsion angles (Vyas et al. 2012). The Ramachandran Plot was provided information on stable conformations of amino acid residues in term of phi (ϕ) and psi (ψ) angels as well as allowed and disallowed region for amino acid residues in high resolution, non-homologous protein crystal structures. Plot points represented the torsion angles of amino acid residues in a three-dimensional protein model.

Pharmacokinetics and drug-likeness predictions

In computer-based drug development, pharmacokinetic, pharmacochemical, and drug-likeness studies have gained a lot of attention; they are used to determine the pharmacological structure by using the website (<https://www.swissadme.ch>). To create SMILES, the chemical structure of cannabinoids was drawn on Marvin and then immediately entered into the webpage to start the prediction process (Daina et al. 2017).

Results and discussion

Binding affinities of protein-ligands interactions

Molecular docking of cannabinoids with some of the proteins (ERK/MEK, and P13K/Akt/mTOR) of cancer pathways and EMT-related proteins (E-cadherin and vimentin) was determined using PyRx software. The maximum binding affinity was exerted by the tetrahydrocannabinol-MEK complex ($-0.8.8$ kcal/mol), and the second highest binding affinity was observed in the cannabidiol-P13K complex ($-0.8.5$ kcal/mol). The binding affinities were increased in order:

cannabigerol < cannabidiol = cannabichromene < tetrahydrocannabivarin (Table 3). Few studies have evidently shown that cannabinoids interact with the MAPK-ERK-ERK signaling pathway and one earlier study depicted that cannabinoids interacted with and downregulated the MAPK-ERK signaling pathway to induce apoptosis in glioma cells (Ellert-Miklaszewska et al. 2005).

Protein–ligand interactions

The current study of *C. sativa* compounds provides promising information on the possible effectiveness of these phytochemicals against cancer. Protein–ligand interactions are crucial to drug development and offer an excellent understanding of the simulation. These protein–ligand interactions fall into four categories: ionic, hydrophobic, hydrogen bonds, and water bridges (ur Rashid et al. 2022). Hydrogen bonding, or H-bonds, is crucial for protein folding and interactions with ligands (Yunta 2017). Table 4 presents the binding interaction of cannabinoids (cannabidiol, tetrahydrocannabivarin, cannabigerol, cannabinol, cannabichromene, tetrahydrocannabinol) with proteins of the MAPK-ERK signaling pathway. ERK1- tetrahydrocannabinol complex was interacted by alkyl bonding with amino acid residues: Cys183, Ile48, Leu173, Val56, and Ala69 at the binding pocket (Fig. 1). Hydrogen bonding interactions were developed by MEK-tetrahydrocannabinol complex with amino acid residues of Lys97 and residues (Phe129, val127,leu118, Ile141, Met143, and Ala220) were developed alky bonding at the active site. Amongst the hydrophobic interactions, pi anion was developed between the MEK-tetrahydrocannabinol complex by Ala220 (Fig. 2). Hydrophobic and hydrogen interactions of tetrahydrocannabinol at binding sites of cannabinoid receptors were reported in the former study and developed interaction by Val, Phe, and Tyr residues at the active site of acetylcholinesterase receptor (Furqan et al. 2020; Aviz-Amador et al. 2021).

P13k-cannabinol was developed H-interaction with amino acid residues Try836, Ile848,cys838, Ile932, and val850 and interacted by covalent bonding (Pi sigma bond) with Met922 residue at binding pockets (Fig. 3). ERK1-cannabinol was developed noncovalent molecular interaction (Pi cation) by Arg189 residue and interacted by covalent bond (alkyl bond) by residues Leu352, Leu86, Arg8, Ile190 at the binding pockets (Fig. 4). Only Akt-cannabinol was found to be interacting via H-bond at the binding site by pro349 residue. An earlier study reported that cannabinol was developed hydrogen and alkyl bonding interaction with cannabinoid receptors (Aviz-Amador et al. 2021).

Table 3 Molecular docking results of cannabinoids-proteins of Pathways of MEK/ERK and P13K/Akt/mTOR, and proteins related to EMT induction

Protein	Vimentin	AKT	E-cadherin	Cannabigerol		ERK1	JNK	P13K	P38	MEK
				mTOR	ERK2					
Binding Affinities (kcal/mole)	-7.3	-6.6	-5.4	-6.7	-6.5	-7.1	-6.7	-6.9	-5.9	-6.3
Protein	Vimentin	AKT	E-cadherin	Cannabichromene		ERK1	JNK	P13K	P38	MEK
				mTOR	ERK2					
Binding Affinities (kcal/mole)	-7.1	-6.9	-6.2	-7.8	-6.7	-7.5	-8	-7.9	-7.1	-7.6
Protein	Vimentin	AKT	E-cadherin	Tetrahydrocannabivarin		ERK1	JNK	P13K	P38	MEK
				mTOR	ERK2					
Binding Affinities (kcal/mole)	-7.6	-6.6	-6.4	-8.3	-7.6	-7.6	-7.9	-7.8	-7.4	-7.8
Protein	Vimentin	AKT	E-cadherin	Cannabinol		ERK1	JNK	P13K	P38	MEK
				mTOR	ERK2					
Binding affinities (kcal/mole)	-7.5	-6.7	-6.9	-7.6	-7.7	-8.3	-7.7	-8.5	-7.6	-8
Protein	Vimentin	AKT	E-cadherin	Cannabidiol		ERK1	JNK	P13K	P38	MEK
				mTOR	ERK2					
Binding affinities (kcal/mole)	-7.1	-6.2	-6.2	-8.2	-7.2	-6.7	-6.8	-7.6	-6.5	-7.4
Protein	Vimentin	AKT	E-cadherin	Tetrahydrocannabinol		ERK1	JNK	P13K	P38	MEK
				mTOR	ERK2					
Binding affinities (kcal/mole)	-7.9	-6.7	-6.5	-8.3	-7.3	-8.6	-7.9	-7.8	-7.5	-8.8

Validation of protein–ligand complex

The protocol of docking was validated by RMSD values and calculated using the PyRx Virtual screening tool. The Root mean square deviation (RMSD) values were calculated by the mean distance between atoms of a position concerning the best fitting position are measured through only movable heavy atoms. The rmsd/lb (the RMSD lower bound) and rmsd/ub (the RMSD upper bound) are two different RMSD metrics that were provided. Two alternatives of RMSD metrics are given, rmsd/ub (RMSD upper bound) and rmsd/lb ((RMSD lower bound), rmsd/ub matches every atom in one conformation with itself in the other conformation. The rmsd/ub values range from 8.6 to 2.0 Å, the computed rmsd/lb values fluctuate between 1.0 and 2.0 Å. These findings suggested that binding complex of cannabinoids (cannabidiol, cannabinol, cannabigerol, tetrahydrocannabinol, tetrahydrocannabivarin, and cannabichromene) with target proteins (Vimentin, mTOR, MEK, Akt, JNK, ERK1/2, P13K, P38, and E-cadherin), who gave the maximum binding energies

was the accurate binding complex. The RMSD values suggested that cannabinoids and protein complexes are valid and accurate and did not face any damage after binding (Table 5). The present results of rmsd/lb also showed the accuracy of the docking methodology employed in this study by the fact that the RMSD value is less than the threshold value of 2.0 established to assess reliability (Benhander and Abdusalam 2022).

Protein structure validation

Plots illustrate specific low energy conformations for ϕ (phi) and ψ (psi) or stable conformations of amino acid residues along with favorable and unfavorable regions for amino acid residues in the plot. The result shows that the number of residues of protein in the allowed region is more than 80%. The number of residues is less than 1% in the disallowed region except ERK1 (1.4%). Some proteins such as E-cadherin, vimentin, Akt, JNK, and P38 have zero residues in the disallowed region (Table 6). This suggests that

Table 4 Amino acid interactions of cannabinoids with target proteins at their active sites

Protein	Cannabigerol					
	Vimentin	Akt	E-cadherin	mTOR	ERK2	ERK1
Alkyl Bond	ALA355, ALA35, MET347, PHE351, VAL389	PHE296, PHE163, PHE359, HIS355, PHE310	ILE4, LYS25	-	LEU105, ALA50, VAL37	LEU360, LEU86, ARG87, PHE348, LEU352
H-Bond	TRY383	-	TRP2, GLU89	UNK252	-	ARG189
Pi-Anion bond	GLU382	-	-	-	ILE29	-
Pi-sigma bond	-	-	-	-	-	-
Pi-Sulphur Bond	-	-	MET92	-	-	-
Cannabichromene						
Protein	Vimentin	Akt	E-cadherin	mTOR	ERK2	ERK1
Alkyl Bond	PHE351, ALA355, VAL389, MET347, LEU387	PHE359, HIS355, PRO314, LYS191, ILE188, PHE163	ALA80, ILE4, MET92	-	LEU154, LEU105, ALA50, VAL37	LEU86, LEU360, LEU352, ARG87
H-Bond	-	-	-	-	-	ILE190
Pi-Anion bond	-	-	-	-	-	-
Pi-Cation bond	-	-	-	-	-	-
Pi-sigma bond	-	-	-	UNK1372	-	HIS195, PHE348
Pi-Sulfur Bond	-	-	-	-	-	-
Tetrahydrocannabivarin						
Protein	Vimentin	Akt	E-cadherin	mTOR	ERK2	ERK1
Alkyl Bond	VAL389, MET347, PHE351, ALA355	PHE350, TYR351, LEU355	ASN168, ILE146	-	ALA50, LYS52, VAL37, LEU154, LEU105, ILE29	LEU86, LEU352
H-Bond	-	-	-	-	-	ILE190
Pi-Anion bond	-	-	-	-	-	-
Pi-Cation bond	-	-	-	-	-	-
Pi-sigma bond	-	-	-	-	-	-
Pi-Sulfur Bond	-	-	-	-	-	-

Table 4 (continued)

Protein	Tetrahydrocannabinol						
	Vimentin	Akt	E-cadherin	mTOR	ERK2	ERK1	JNK
H-Bond	-	-	-	-	MET106	-	-
Pi-Anion bond	-	-	-	-	-	-	-
Pi-Cation bond	-	-	-	-	ARG18, ARG87	-	-
Pi-sigma bond	-	-	-	UNK248, UNK120	-	VAL158	-
Pi-Sulphur Bond	-	-	-	-	-	-	-
Cannabinol							
Protein	Vimentin	Akt	E-cadherin	mTOR	ERK2	ERK1	JNK
Alkyl Bond	ARG378, TYR358	PHE350, LEU361,	ALA80, MET92, TYR36, ILE24, TRP2	-	LEU154, CYS164, ALA50, ILE82	LEU352, LEU86, ARG87, ILE190	MET149, ILE124, ALA91, LEU206
H-Bond	-	PRO349	-	-	-	-	-
Pi-Anion bond	GLU375	-	-	-	-	-	-
Pi-Cation bond	-	-	-	-	ARG189	-	-
Pi-sigma bond	ILE362	TYR351	-	UNK538, UNK642	ILE29	PHE348	VAL196, VAL78
Pi-Sulfur Bond	-	-	-	-	-	-	MET146
Cannabidiol							
Protein	Vimentin	Akt	E-cadherin	mTOR	ERK2	ERK1	JNK
Alkyl Bond	LEU168, VAL158, LEU110, ALA42	PHE163, LYS191, PHE310	ALA80, TYR36, MET92, ILE24	-	LYS52, VAL37, ALA33, ILE29, ALA50, LEU154	ALA349, LEU363, PHE346, PHE398	LEU168, VAL158, LEU110, ALA42
H-Bond	ILE32	-	-	-	-	-	ILE32
Pi-Anion bond	-	-	-	-	LEU154	GLU367	-
Pi-Cation bond	-	-	-	-	-	-	-
Pi-sigma bond	-	-	-	UNK570	-	-	-
Pi-Sulphur Bond	-	-	-	-	-	-	-
P38							
Protein	Vimentin	Akt	E-cadherin	mTOR	ERK2	ERK1	JNK
Alkyl Bond	LEU168, VAL158, LEU110, ALA42	PHE163, LYS191, PHE310	ALA80, TYR36, MET92, ILE24	-	LYS52, VAL37, ALA33, ILE29, ALA50, LEU154	ALA349, LEU363, PHE346, PHE398	LEU168, VAL158, LEU110, ALA42
H-Bond	ILE32	-	-	-	-	-	ILE32
Pi-Anion bond	-	-	-	-	LEU154	GLU367	-
Pi-Cation bond	-	-	-	-	-	-	-
Pi-sigma bond	-	-	-	UNK570	-	-	-
Pi-Sulphur Bond	-	-	-	-	-	-	-
P13K							
Protein	Vimentin	Akt	E-cadherin	mTOR	ERK2	ERK1	JNK
Alkyl Bond	LEU168, VAL158, LEU110, ALA42	PHE163, LYS191, PHE310	ALA80, TYR36, MET92, ILE24	-	LYS52, VAL37, ALA33, ILE29, ALA50, LEU154	ALA349, LEU363, PHE346, PHE398	LEU168, VAL158, LEU110, ALA42
H-Bond	ILE32	-	-	-	-	-	ILE32
Pi-Anion bond	-	-	-	-	LEU154	GLU367	-
Pi-Cation bond	-	-	-	-	-	-	-
Pi-sigma bond	-	-	-	UNK570	-	-	-
Pi-Sulphur Bond	-	-	-	-	-	-	-
MEK							
Protein	Vimentin	Akt	E-cadherin	mTOR	ERK2	ERK1	JNK
Alkyl Bond	LEU168, VAL158, LEU110, ALA42	PHE163, LYS191, PHE310	ALA80, TYR36, MET92, ILE24	-	LYS52, VAL37, ALA33, ILE29, ALA50, LEU154	ALA349, LEU363, PHE346, PHE398	LEU168, VAL158, LEU110, ALA42
H-Bond	ILE32	-	-	-	-	-	ILE32
Pi-Anion bond	-	-	-	-	LEU154	GLU367	-
Pi-Cation bond	-	-	-	-	-	-	-
Pi-sigma bond	-	-	-	UNK570	-	-	-
Pi-Sulphur Bond	-	-	-	-	-	-	-
ARG136							
Protein	Vimentin	Akt	E-cadherin	mTOR	ERK2	ERK1	JNK
Alkyl Bond	LEU168, VAL158, LEU110, ALA42	PHE163, LYS191, PHE310	ALA80, TYR36, MET92, ILE24	-	LYS52, VAL37, ALA33, ILE29, ALA50, LEU154	ALA349, LEU363, PHE346, PHE398	LEU168, VAL158, LEU110, ALA42
H-Bond	ILE32	-	-	-	-	-	ILE32
Pi-Anion bond	-	-	-	-	LEU154	GLU367	-
Pi-Cation bond	-	-	-	-	-	-	-
Pi-sigma bond	-	-	-	UNK570	-	-	-
Pi-Sulphur Bond	-	-	-	-	-	-	-
VAL627, PHE688, ALA637, CYS689, VAL670, LYS737							
Protein	Vimentin	Akt	E-cadherin	mTOR	ERK2	ERK1	JNK
Alkyl Bond	LEU168, VAL158, LEU110, ALA42	PHE163, LYS191, PHE310	ALA80, TYR36, MET92, ILE24	-	LYS52, VAL37, ALA33, ILE29, ALA50, LEU154	ALA349, LEU363, PHE346, PHE398	LEU168, VAL158, LEU110, ALA42
H-Bond	ILE32	-	-	-	-	-	ILE32
Pi-Anion bond	-	-	-	-	LEU154	GLU367	-
Pi-Cation bond	-	-	-	-	-	-	-
Pi-sigma bond	-	-	-	UNK570	-	-	-
Pi-Sulphur Bond	-	-	-	-	-	-	-

Table 4 (continued)

Protein	Tetrahydrocannabinol						
	mTOR	ERK2	ERK1	JNK	PI3K	P38	MEK
Alkyl Bond	-	LEU105, VAL37, ALA50, LYS52, CYS164	CYS183, ILE48, LEU173, VAL56, ALA69	MET108, VAL40, LYS55, LEU168	PRO449, PRO447	LYS165	PHE129, VAL127, LEU118, ILE141, MET143, ALA220
H-Bond	-	-	-	-	-	LEU164, GLU81, GLN133	LYS97
Pi-Anion bond	-	-	-	-	-	-	-
Pi-Cation bond	-	-	-	-	-	-	-
Pi-sigma bond	-	ILE29	-	LEU168	-	-	-
Pi-Sulfur Bond	-	-	-	-	-	-	-

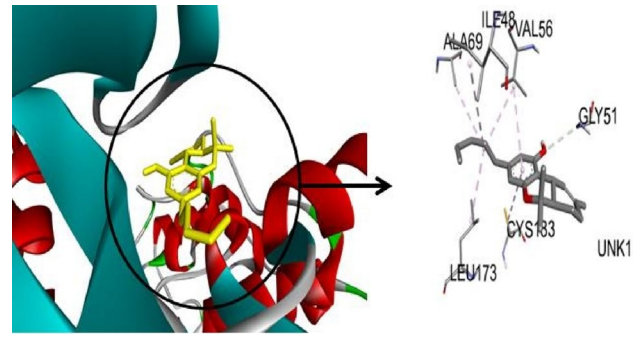


Fig. 1 3D visualization of ERK1-Tetrahydrocannabinol

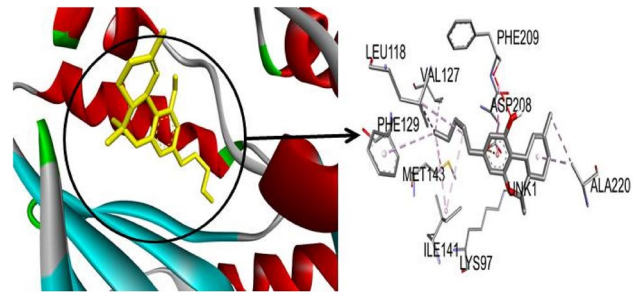


Fig. 2 3D visualization of MEK-Tetrahydrocannabinol

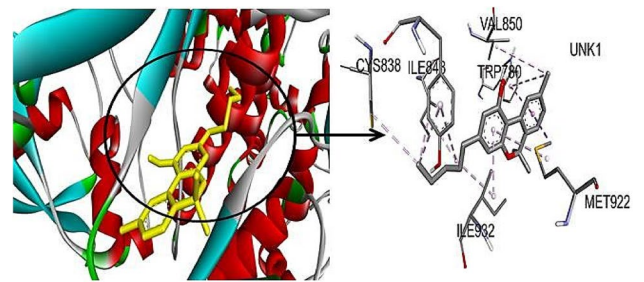


Fig. 3 3D visualization of PI3K-Cannabinol

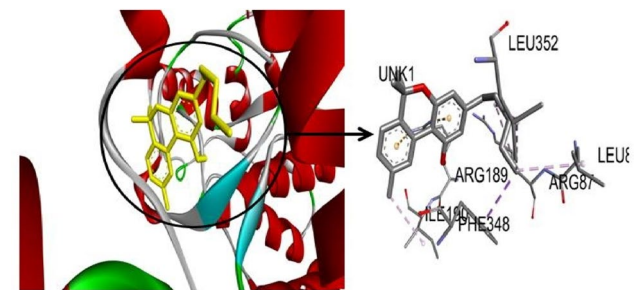


Fig. 4 3D visualization of ERK1-Cannabinol

Table 5 Root mean square deviation (RMSD) values, which indicate the average distance between atoms at a point in relation to the best fitting position

PROTEIN–LIGAND	Distance from Best Mode	
	RMSD/Upper Bound	RMSD/Lower Bound
Vimentin-Tetrahydrocannabinol	3.828	1.582
Vimentin –cannabidiol	2.234	1.036
Vimentin –cannabichromene	5.461	1.897
Vimentin –cannabinol	6.997	1.777
Vimentin –cannabigerol	2.52	1.784
Vimentin –Terahydrocannabivarin	3.884	1.744
mTOR-Tetrahydrocannabinol	1.671	1.304
mTOR-cannabidiol	4.179	1.792
mTOR-cannabichromene	4.317	1.752
mTOR-cannabinol	6.886	1.937
mTOR-cannabigerol	2.339	1.255
mTOR-Terahydrocannabivarin	2.486	1.567
MEK-Tetrahydrocannabinol	3.28	1.43
MEK-cannabidiol	3.11	1.03
MEK-cannabichromene	4.55	1.89
MEK-cannabinol	5.027	1.729
MEK-cannabigerol	2.776	1.814
MEK-Terahydrocannabivarin	5.861	1.604
JNK-Tetrahydrocannabinol	2.098	1.733
JNK-cannabidiol	3.19	1.194
JNK-cannabichromene	3.468	1.435
JNK-cannabinol	3.468	1.435
JNK-cannabigerol	2.27	1.483
JNK-Terahydrocannabivarin	5.094	1.69
ERK2-Tetrahydrocannabinol	6.95	1.962
ERK2-cannabidiol	4.649	1.787
ERK2-cannabichromene	5.493	1.865
ERK2-cannabinol	3.724	1.557
ERK2-cannabigerol	2.964	1.256
ERK2-Terahydrocannabivarin	6.242	1.749
ERK1-Tetrahydrocannabinol	6.849	1.985
ERK1-cannabidiol	4.178	1.906
ERK1-cannabichromene	7.816	1.391
ERK1-cannabinol	6.576	1.198
ERK1-cannabigerol	8.642	1.59
ERK1-Terahydrocannabivarin	6.353	1.76
Akt-Tetrahydrocannabinol	6.888	1.36
Akt-cannabidiol	5.241	1.61
Akt-cannabichromene	8.272	1.57
Akt-cannabinol	6.495	1.43
Akt-cannabigerol	2.273	1.04
Akt-Terahydrocannabivarin	6.743	1.67
P13K-Tetrahydrocannabinol	4.833	1.39
P13K-cannabidiol	6.315	1.56
P13K-cannabichromene	7.269	1.39
P13K-cannabinol	7.644	1.88
P13K-cannabigerol	2.024	1.52

Table 5 (continued)

PROTEIN–LIGAND	Distance from Best Mode	
	RMSD/Upper Bound	RMSD/Lower Bound
P13K-Tetrahydrocannabivarin	6.049	1.69
P38-Tetrahydrocannabinol	5.115	1.69
P38-cannabidiol	2.243	1.24
P38-cannabichromene	3.981	1.51
P38-cannabinol	3.802	1.59
P38-cannabigerol	5.155	1.95
P38-Tetrahydrocannabivarin	2.996	1.54
E-cadherin-Tetrahydrocannabinol	2.545	1.45
E-cadherin-cannabidiol	2.656	1.70
E-cadherin-cannabichromene	4.378	2.06
E-cadherin-cannabinol	2.379	1.31
E-cadherin-cannabigerol	3.975	1.52
E-cadherin-Tetrahydrocannabivarin	3.943	1.77

the optimized protein structure of MEK, ERK1/2/, P38, P13K, mTOR, Akt, E-cadherin, and vimentin are suitable for molecular docking and the respective ligands can interact at their binding pockets with stable binding. The majority of points of the Ramachandran plots are situated in favorable regions, suggesting that the majority of the dihedral angles of amino acid residues are in appropriate ranges that assisted to develop stable protein–ligand complex (Hollingsworth and Karplus 2010).

The regions in the red indicates favoured region, yellow for allowed region, light yellow for generously allowed region of amino ac

Drug-likeness predictions and pharmacokinetics

The in silico pharmacokinetic and drug-likeness properties of the six cannabinoids from the leaves of *C. sativa* are reported (Table 7) and the values were predicted by the SwissADME. Lipinski's rule of five, which states that if any small molecule violates more than two of these criteria (molecular weight ≤ 500 g/mol, number of hydrogen bond donors ≤ 5 , number of hydrogen bond acceptors ≤ 10 , calculated $\log P \leq 5$), the molecule is said to be impermeable or badly absorbed (Lipinski et al. 1997). This rule was used to predict the drug-likeness of the cannabinoid compounds (Table 7). The cannabinoids have 1 violation ($MLOGP > 4.15$) of the Lipinski rules of five except tetrahydrocannabivarin (0 violation). All cannabinoids have a good bioavailability score (0.55) that verifies their drug-likeness properties of cannabinoids (Ibrahim et al. 2021). Six cannabinoids meet the requirements for leadlikeness that is, a molecular entity that can be optimized (Teague et al. 1999).

However, the synthetic accessibility value of these cannabinoids is less than 6, which suggests their possibility to be synthesized. The primary concept of the SwissADME Synthetic Accessibility (SA) Score is that synthesis ease is correlated with the frequency of molecular fragments in "really" attainable compounds and the score ranges from 1 (very easy to synthesize) to 10 (very hard to synthesize) (Ertl and Schuffenhauer 2009). Furthermore, only tetrahydrocannabivarin has less than 5 values of Consensus Log Po/w which is an average of the five lipophilicity predictions, falling within an acceptable range (Alminderej et al. 2020). According to Lipinski's rule of five, the range of total polar surface area (TPSA) should be of 0–140 that is benchmark for anticancer drugs and cannabinoids are compliance with Lipinski's rule of five. The TPSA of all the compounds was between 29.46 and 40.46 Å² (Jagannathan 2019). Cannabigerol, cannabichromene, tetrahydrocannabivarin, cannabinol, cannabidiol, and tetrahydrocannabinol have numerous rotatable bonds, which are less than 10. This indicates that these compounds have stable conformation and bioavailable if consumed orally (Rai et al. 2023).

The current state of drug development is characterized by pharmacokinetic and safety profiles of novel chemical entities (NCE) (Chen et al. 2018). In the early stages of drug development, several computational techniques could assist us in making predictions about the drug-likeness activity and possible toxicity of novel molecules. The ADMESwiss predicted that all six cannabinoid compounds would be highly absorbed via the intestine.

Predictions were made for the pharmacokinetic characteristics of absorption, distribution, skin penetration, metabolism, biotransformation, and excretion. This prediction tool

Table 6 Ramachandran plot of each protein shows the overview of allowed and disallowed regions of torsion angle values,

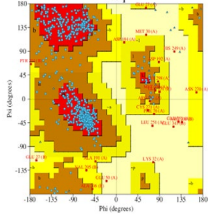
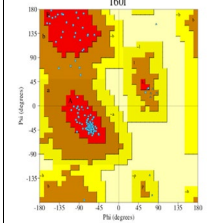
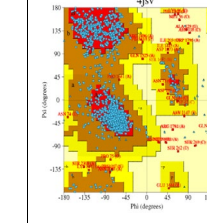
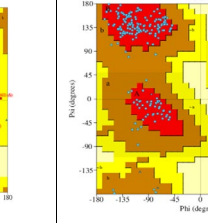
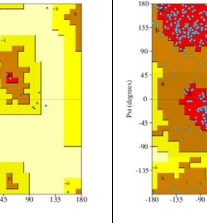
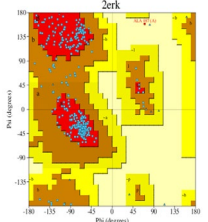
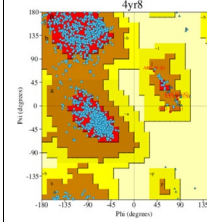
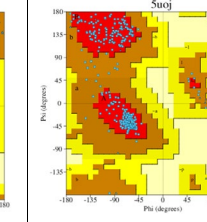
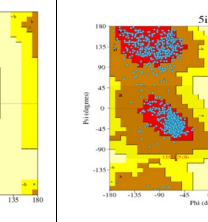
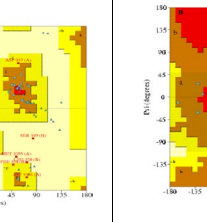
									
ERK1		Akt		mTO		E-cadherin		MEK	
Allowed region	81.7%	Allowed region	95.2%	Allowed region	85.9%	Allowed region	90.2%	Allowed region	91.3%
Additional allowed region	14.6%	Additional allowed region	4.8%	Additional allowed region	11.9%	Additional allowed region	9.8%	Additional allowed region	8.1%
Generously allowed region	2.2%	Generously allowed region	0.0%	Generously allowed region	1.4%	Generously allowed region	0.0%	Generously allowed region	0.2%
Disallowed region	1.4%	Disallowed region	0.0%	Disallowed region	0.09%	Disallowed region	0.0%	Disallowed region	0.4%
									
ERK2		JNK		P38		P13K		Vimentin	
Allowed region	85.7%	Allowed region	90.3%	Allowed region	90.6%	Allowed region	90.0%	Allowed region	96.7%
Additional allowed region	14.0%	Additional allowed region	9.4%	Additional allowed region	9.4%	Additional allowed region	9.4%	Additional allowed region	3.3%
Generously allowed region	0.0%	Generously allowed region	0.3%	Generously allowed region	0.0%	Generously allowed region	0.4%	Generously allowed region	0.0%
Disallowed region	0.3%	Disallowed region	0.0%	Disallowed region	0.0%	Disallowed region	0.3%	Disallowed region	0.0%

Table 7 Physicochemical parameters of cannabinoids leaves of *Cannabis sativa* using SwissADME

Properties	Cannabigerol	Cannabichromene	Tetrahydrocannabivarin	Cannabinol	Cannabidiol	Tetrahydrocannabinol
Physiochemical						
Molecular weight	316.48 g/mol	314.46 g/mol	286.41 g/mol	310.43 g/mol	314.46 g/mol	314.46 g/mol
Num. of rotatable bonds	9	7	2	4	6	4
Num. H-bond acceptors	2	2	2	2	2	2
Num. H-bond donors	2	1	1	1	2	1
Consensus Log Po/w	5.74	5.74	4.68	5.21	5.2	5.33
TPSA	40.46 Å ²	29.46 Å ²	29.46 Å ²	29.46 Å ²	40.46 Å ²	29.46 Å ²
Drug Likeness	Yes; 1 violation: MLOGP > 4.15	Yes; 1 violation: MLOGP > 4.15	Yes; 0 violation	Yes; 1 violation: MLOGP > 4.15	Yes; 1 violation: MLOGP > 4.15	Yes; 1 violation: MLOGP > 4.15
Bioavailability Score	0.55	0.55	0.55	0.55	0.55	0.55
Medicinal Chemistry Lead Likeness	No; 2 violations: Rotors > 7, XLOGP3 > 3.5	No; 1 violation: XLOGP3 > 3.5	No; 1 violation: XLOGP3 > 3.5	No; 1 violation: XLOGP3 > 3.5	No; 1 violation: XLOGP3 > 3.5	No; 1 violation: XLOGP3 > 3.5
Synthetic accessibility	3.14	4.26	4.05	3.39	4.05	4.27

suggests that tetrahydrocannabinol, tetrahydrocannabivarin, cannabidiol, and tetrahydrocannabinol except cannabichromene and cannabigerol can cross the blood–brain barrier. This prediction makes it clear that every component had high GI absorption, as seen in Table 7. The chemicals that are blood–brain permeant may, upon metabolism, produce

toxicants that are damaging to the brain and bloodstream. Potential medications for transdermal and oral delivery can be identified and predicted using the skin permeability model. Cannabigerol was discovered to be the cannabinoid more skin permeant. According to the model, a molecule is considered less skin permeant if its log Kp value is more

Table 8 Pharmacokinetics parameters of cannabinoids leaves of *Cannabis sativa* using by SwissADME

Parameters of pharmacokinetics	Tetrahydrocannabivarin	Cannabigerol	Cannabinol	Tetrahydrocannabinol	Cannabichromene	Canabidiol
GI absorption	High	High	High	High	High	High
BBB permeant	Yes	No	Yes	Yes	No	Yes
P-gp substrate	No	No	No	No	No	No
CYP1A2 inhibitor	No	Yes	No	No	No	No
CYP2C19 inhibitor	No	Yes	No	No	No	Yes
CYP2C9 inhibitor	No	No	No	No	Yes	Yes
CYP2D6 inhibitor	No	No	No	No	No	No
CYP3A4 inhibitor	No	No	No	No	No	No
Log Kp (skin permeation)	- 3.87 cm/s	- 2.96 cm/s	- 3.86 cm/s	- 3.27 cm/s	- 3.35 cm/s	- 3.59 cm/s

negative which supports the present findings (Daina et al. 2017).

The potential for cannabinoids to function as either a substrate or an inhibitor of P-gp was assessed; the findings showed that cannabinoids are not substrates of P-gp.

An earlier study reported if there is no P-glycoprotein (P-gp) substrate that suggests the compound has high bioavailability and intestinal absorption, this supports present findings (Montanari and Ecker 2015). Prediction reveals that cannabinoids are substrate of CYP1A2

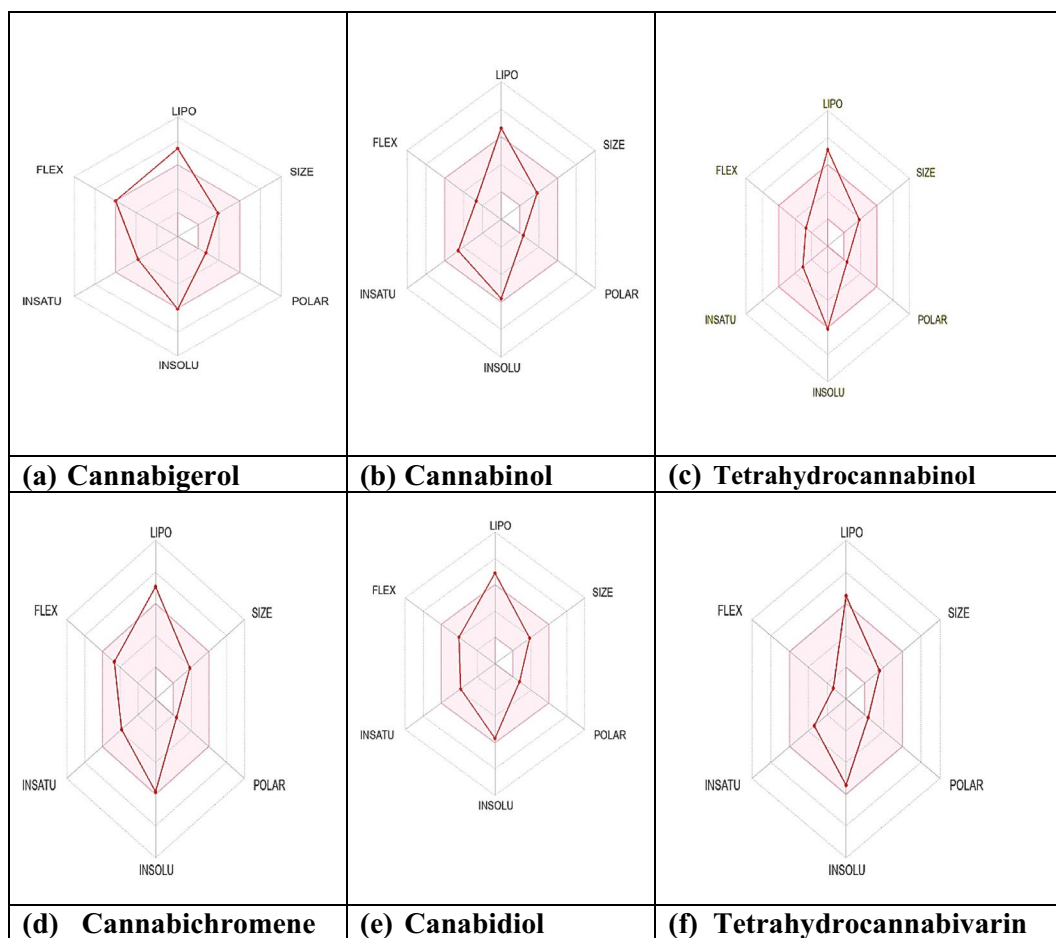


Fig. 5 Bioavailability radars (a–f)

(except cannabigerol), CYP2C19 (except cannabigerol and cannabidiol), CYP2C9 (except cannabichromene and cannabidiol), CYP2D6, and CYP3A4 (Table 8). Previous Cytochrome P450 (CYP) enzymes play a crucial role in drug removal through metabolic transformation, making molecule-enzyme interactions critical (Daina et al. 2017). Because inhibition of these isoenzymes reduces the solubility and accumulation of the drug or its metabolites, it may have unintended negative side effects (Mishra and Dahima 2019).

All characteristics, including XLOGP3 (-0.7 to + 5.0), Molecular weight (150 to 500 g/mol), Solubility (log S not exceeding 6), and Flexibility (FLEX) (not exceeding 9 rotatable bonds), are within the permissible range, according to the bioavailability radar (Fig. 5). The present finding fall within the standard drug flexibility and solubility criteria according to that Log S for solubility should not be greater than 6. XLOGP3 for lipophilicity should fall between -0.7 to + 6.0. The molecule should have no more than 9 rotatable bonds for flexibility (Cheng et al. 2012). The drug-likeness and drug score of cannabinoids suggest that they are better suited for usage as medicines.

Conclusion

This study docked six cannabinoids from *Cannabis sativa* with proteins related to MAPK-ERK signaling pathways and proteins related to epithelial-mesenchymal transition (EMT) induction. The pharmacokinetics and drug-likeness properties of six cannabinoids (tetrahydrocannabivarin, cannabigerol, cannabiol, cannabidiol, tetrahydrocannabinol, and cannabichromene) from *C. sativa* leaves were also analyzed. All the cannabinoids had expressed good binding affinities and their drug-likeness as well as pharmacokinetics elucidated that they may be used as active drugs or inhibitors to downregulate Akt, mTOR, JNK, MEK, P38, P13K, ERK1/2, vimentin, E-cadherin. According to drug-likeness, pharmacokinetic, and binding affinities, out of the six cannabinoids, tetrahydrocannabinol and cannabiol may be the best inhibitors of proteins related to the MAPK-ERK signaling pathway and EMT induction. This shows that cannabinoids may be used to formulate excellent anticancer medications. The study suggests that cannabinoids are better suited as drugs and to acquire a better knowledge of these medications, improve safe use, and effective prescribing, more clinical research in the actual patient groups for whom prescribing may be considered is required.

Supplementary Information The online version contains supplementary material available at <https://doi.org/10.1007/s40203-024-00213-4>.

Author contributions Shabnoor Iqbal, Writing of Original Draft, and data analysis. Motlalepula Matsabisa, Supervision, Validation.

Funding Open access funding provided by University of the Free State. The author(s) received no financial support for the authorship, the research, or the publication.

Data availability Data is available in manuscript as well as supplementary file and any additional data will be available on request.

Declarations

Conflict of Interest The authors declared no conflict of interest.

Open Access This article is licensed under a Creative Commons Attribution 4.0 International License, which permits use, sharing, adaptation, distribution and reproduction in any medium or format, as long as you give appropriate credit to the original author(s) and the source, provide a link to the Creative Commons licence, and indicate if changes were made. The images or other third party material in this article are included in the article's Creative Commons licence, unless indicated otherwise in a credit line to the material. If material is not included in the article's Creative Commons licence and your intended use is not permitted by statutory regulation or exceeds the permitted use, you will need to obtain permission directly from the copyright holder. To view a copy of this licence, visit <http://creativecommons.org/licenses/by/4.0/>.

References

- Alminderej F, Bakari S, Almundarij TI, Snoussi M, Aouadi K, Kadri A (2020) Antioxidant activities of a new chemotype of *Piper cubeba* L. fruit essential oil (Methyleugenol/Eugenol): in silico molecular docking and ADMET studies. *Plants* 9:1534. <https://doi.org/10.3390/plants9111534>
- Aviz-Amador A, Contreras-Puentes N, Mercado-Camargo J (2021) Virtual screening using docking and molecular dynamics of cannabinoid analogs against CB1 and CB2 receptors. *Comput Biol Chem* 95:107590. <https://doi.org/10.1016/j.compbiolchem.2021.107590>
- Beach JR, Hussey GS, Miller TE, Chaudhury A, Patel P, Monslow J, Zheng Q, Keri RA, Reizes O, Bresnick AR (2011) Myosin II isoform switching mediates invasiveness after TGF- β -induced epithelial-mesenchymal transition. *Proc Natl Acad Sci* 108:17991–17996. <https://doi.org/10.1073/pnas.1106499108>
- Benhander GM, Abdusalam AAA (2022) Identification of potential inhibitors of SARS-CoV-2 main protease from *Allium roseum* L. molecular docking study. *Chem Afr* 5:57–67. <https://doi.org/10.1007/s42250-021-00296-y>
- Castaneto MS, Gorelick DA, Desrosiers NA, Hartman RL, Pirard S, Huestis MA (2014) Synthetic cannabinoids: epidemiology, pharmacodynamics, and clinical implications. *Drug Alcohol Depend* 144:12–41. <https://doi.org/10.1016/j.drugalcdep.2014.08.005>
- Chen J, Luo X, Qiu H, Mackey V, Sun L, Ouyang X (2018) Drug discovery and drug marketing with the critical roles of modern administration. *Am J Trans Res* 10:4302
- Cheng F, Li W, Zhou Y, Shen J, Wu Z, Liu G, Lee PW, Tang Y (2012) admetSAR: a comprehensive source and free tool for assessment of chemical ADMET properties. *ACS Publ* 52(11):3099–3105. <https://doi.org/10.1021/ci300367a>
- Cohen K, Weinstein AM (2018) Synthetic and non-synthetic cannabinoid drugs and their adverse effects—a review from public health prospective. *Front Public Health* 6:162. <https://doi.org/10.3389/fpubh.2018.00162>
- Daina A, Michielin O, Zoete V (2017) SwissADME: a free web tool to evaluate pharmacokinetics, drug-likeness and medicinal chemistry

- friendliness of small molecules. *Sci Rep* 7:42717. <https://doi.org/10.1038/srep42717>
- Dehelean CA, Marcovici I, Soica C, Mioc M, Coricovac D, Iurciuc S, Cretu OM, Pinzaru I (2021) Plant-derived anticancer compounds as new perspectives in drug discovery and alternative therapy. *Molecules*. <https://doi.org/10.3390/molecules26041109>
- Ellert-Miklaszewska A, Kaminska B, Konarska L (2005) Cannabinoids down-regulate PI3K/Akt and Erk signalling pathways and activate proapoptotic function of Bad protein. *Cell Signal* 17:25–37. <https://doi.org/10.1016/j.cellsig.2004.05.011>
- Emhemmed F, Zhao M, Yorulmaz S, Steyer D, Leitao C, Alignan M, Cerny M, Paillard A, Delacourt FM, Julien-David D (2022) Cannabis sativa extract induces apoptosis in human pancreatic 3D cancer models: Importance of major antioxidant molecules present therein. *Molecules* 27:1214. <https://doi.org/10.3390/molecules27041214>
- Ertl P, Schuffenhauer A (2009) Estimation of synthetic accessibility score of drug-like molecules based on molecular complexity and fragment contributions. *J Cheminf* 1:1–11. <https://doi.org/10.1186/1758-2946-1-8>
- Farhan M, Wang H, Gaur U, Little PJ, Xu J, Zheng W (2017) FOXO signaling pathways as therapeutic targets in cancer. *Int J Biol Sci* 13:815. <https://doi.org/10.7150/ijbs.20052>
- Furqan T, Batool S, Habib R, Shah M, Kalasz H, Darvas F, Kuca K, Nepovimova E, Batool S, Nurulain SM (2020) Cannabis constituents and acetylcholinesterase interaction: molecular docking, in vitro studies and association with CNR1 rs806368 and ACHE rs17228602. *Biomolecules* 10:758. <https://doi.org/10.3390/biom10050758>
- Hamidi AA, Khalili-Tanha G, Nasrpour Navaei Z, Moghbeli M (2022) Long non-coding RNAs as the critical regulators of epithelial mesenchymal transition in colorectal tumor cells: an overview. *Cancer Cell Int* 22:1–15. <https://doi.org/10.1186/s12935-022-02501-5>
- Hollingsworth SA, Karplus PA (2010) A fresh look at the Ramachandran plot and the occurrence of standard structures in proteins. *Biomol Concepts* 1:271–283. <https://doi.org/10.1515/BMC.2010.022>
- Huang Y, Hong W, Wei X (2022) The molecular mechanisms and therapeutic strategies of EMT in tumor progression and metastasis. *J Hematol Oncol* 15:129. <https://doi.org/10.1186/s13045-022-01347-8>
- Ibrahim MT, Uzairu A, Shallangwa GA, Uba S (2021) Molecular docking investigation and pharmacokinetic properties prediction of some anilinopyrimidines analogues as egfr t790m tyrosine kinase inhibitors. *Egypt J Basic Appl Sci* 8:203–213. <https://doi.org/10.1080/2314808X.2021.1946650>
- Jagannathan R (2019) Characterization of drug-like chemical space for cytotoxic marine metabolites using multivariate methods. *ACS Omega* 4:5402–5411. <https://doi.org/10.1021/acsomega.8b01764>
- Johnson SM, Gulhati P, Rampy BA, Han Y, Rychahou PG, Doan HQ, Weiss HL, Evers BM (2010) Novel expression patterns of PI3K/Akt/mTOR signaling pathway components in colorectal cancer. *J Am Coll Surg* 210:767–776. <https://doi.org/10.1016/j.jamcollsurg.2009.12.008>
- Lipinski CA, Lombardo F, Dominy BW, Feeney PJ (1997) Experimental and computational approaches to estimate solubility and permeability in drug discovery and development settings. *Adv Drug Deliv Rev* 23:3–25. [https://doi.org/10.1016/S0169-409X\(96\)00423-1](https://doi.org/10.1016/S0169-409X(96)00423-1)
- Mishra S, Dahima R (2019) In vitro ADME studies of TUG-891, a GPR-120 inhibitor using SWISS ADME predictor. *J Drug Deliv Therap* 9:366–369. <https://doi.org/10.22270/jddt.v9i2-s.2710>
- Montanari F, Ecker GF (2015) Prediction of drug–ABC-transporter interaction—recent advances and future challenges. *Adv Drug Deliv Rev* 86:17–26. <https://doi.org/10.1016/j.addr.2015.03.001>
- Navaei ZN, Khalili-Tanha G, Zangouei AS, Abbaszadegan MR, Moghbeli M (2021) PI3K/AKT signaling pathway as a critical regulator of Cisplatin response in tumor cells. *Oncol Res* 29:235. <https://doi.org/10.32604/or.2022.025323>
- Pan G, Liu Y, Shang L, Zhou F, Yang S (2021) EMT-associated microRNAs and their roles in cancer stemness and drug resistance. *Cancer Commun* 41:199–217. <https://doi.org/10.1002/cac2.12138>
- Rai M, Singh AV, Paudel N, Kanase A, Falletta E, Kerkar P, Heyda J, Barghash RF, Pratap Singh S, Soos M (2023) Herbal concoction Unveiled: a computational analysis of phytochemicals' pharmacokinetic and toxicological profiles using novel approach methodologies (NAMs). *Curr Res Toxicol* 5:100118. <https://doi.org/10.1016/j.crtox.2023.100118>
- Serrano-Gomez SJ, Maziveyi M, Alahari SK (2016) Regulation of epithelial-mesenchymal transition through epigenetic and post-translational modifications. *Mol Cancer* 15:1–14. <https://doi.org/10.1186/s12943-016-0502-x>
- Sugiura R, Satoh R, Takasaki T (2021) ERK: a double-edged sword in cancer. ERK-dependent apoptosis as a potential therapeutic strategy for cancer. *Cells* 10:2509. <https://doi.org/10.3390/cells10102509>
- Teague SJ, Davis AM, Leeson PD, Oprea T (1999) The design of lead-like combinatorial libraries. *Angew Chem Int Ed* 38:3743–3748. [https://doi.org/10.1002/\(sici\)1521-3773\(19991216\)38:24%3C3743::aid-anie3743%3E3.0.co;2-u](https://doi.org/10.1002/(sici)1521-3773(19991216)38:24%3C3743::aid-anie3743%3E3.0.co;2-u)
- Tomko AM, Whynot EG, Ellis LD, Dupre DJ (2020) Anti-cancer potential of cannabinoids, terpenes, and flavonoids present in Cannabis. *Cancers*. <https://doi.org/10.3390/cancers12071985>
- ur Rashid H, Ahmad N, Abdalla M, Khan K, Martines MAU, Shabana S (2022) Molecular docking and dynamic simulations of Cefixime, Etoposide and Nebrodenside A against the pathogenic proteins of SARS-CoV-2. *J Mol Struct* 1247:131296. <https://doi.org/10.1016/j.molstruc.2021.131296>
- Vyas VK, Ukawala RD, Ghate M, Chintha C (2012) Homology modeling a fast tool for drug discovery: current perspectives. *Indian J Pharm Sci* 74:1–17. <https://doi.org/10.4103/0250-474x.102537>
- Wei R, Xiao Y, Song Y, Yuan H, Luo J, Xu W (2019) FAT4 regulates the EMT and autophagy in colorectal cancer cells in part via the PI3K-AKT signaling axis. *J Exp Clin Cancer Res* 38:1–14. <https://doi.org/10.1186/s13046-019-1043-0>
- Yunta MJ (2017) It is important to compute intramolecular hydrogen bonding in drug design. *Am J Model Optim* 5:24–57. <https://doi.org/10.12691/ajmo-5-1-3>

Publisher's Note Springer Nature remains neutral with regard to jurisdictional claims in published maps and institutional affiliations.